

Submitted to ApJ: Feb 4, 2011. Accepted: Mar 15, 2011

THE IMPACT OF THE CONVECTIVE BLUESHIFT EFFECT ON SPECTROSCOPIC PLANETARY TRANSITS

Avi Shporer^{1,2}, Tim Brown^{1,2}

ABSTRACT

We present here a small anomalous radial velocity (RV) signal expected to be present in RV curves measured during planetary transits. This signal is induced by the convective blueshift (CB) effect — a net blueshift emanating from the stellar surface, resulting from a larger contribution of rising hot and bright gas relative to the colder and darker sinking gas. Since the CB radial component varies across the stellar surface, the light blocked by the planet during a transit will have a varying RV component, resulting in a small shift of the measured RVs. The CB-induced anomalous RV curve is different than, and independent of, the well known Rossiter-McLaughlin (RM) effect, where the latter is used for determining the sky-projected angle between the host star rotation axis and the planet’s orbital angular momentum axis. The observed RV curve is the sum of the CB and RM signals, and they are both superposed on the orbital Keplerian curve. If not accounted for, the presence of the CB RV signal in the spectroscopic transit RV curve may bias the estimate of the spin-orbit angle. In addition, future very high precision RVs will allow the use of transiting planets to study the CB of their host stars.

Subject headings: planetary systems

1. Introduction

Radial velocity (RV) measurements of Sun-like stars are now reaching the 1 m s^{-1} accuracy milestone and are expected to become more accurate in the future (e.g., Li et al. 2008;

¹Las Cumbres Observatory Global Telescope Network, 6740 Cortona Drive, Suite 102, Santa Barbara, CA 93117, USA; ashporer@lcogt.net

²Department of Physics, Broida Hall, University of California, Santa Barbara, CA 93106, USA

Dumusque et al. 2010; Howard et al. 2010; Lo Curto et al. 2010). Naturally, the increased sensitivity allows to identify more and more low amplitude effects that need to be accounted for when modeling the measured RV curves. We present here such an effect, induced by what is known as stellar convective blueshift (hereafter CB; explained in more detail below), which manifests itself as a small anomalous RV signal during a planetary transit.

This small RV signal is superposed on, and independent of, the already well known Rossiter-McLaughlin (RM) effect (Rossiter 1924; McLaughlin 1924; see also Holt 1893), seen during a planetary transit (e.g., Queloz et al. 2000; Winn et al. 2005). The RM effect originates from the host star rotation, and allows the measurement of λ , the sky-projected angle between the host star’s rotation axis and the planet’s orbital angular momentum¹, which is an important piece of information in the study of planetary formation and orbital evolution (e.g., Fabrycky & Tremaine 2007; Triaud et al. 2010; Winn et al. 2010). During transit the planet blocks the light coming from different regions of the host star surface, with a different RV component due to the star’s rotation. The observed line profile is distorted, it becomes asymmetric, and its center is shifted, resulting in the RM RV signal. The RM RV curve shape depends primarily on the spin-orbit angle λ , the sky-projected rotation velocity V_{rot} , and the planet to star radii ratio $r \equiv R_p/R_s$ (Gaudi & Winn 2007).

The new effect we present here is expected to be at the 1 m s^{-1} level and to occur during transit, thus affecting the interpretation of the RV curve. We describe the CB effect in Section 2, and in Section 3 we use a simple numerical model to calculate the impact of the CB effect on RVs measured during transit. We give a discussion in Section 4 and a summary in Section 5.

2. The Convective Blueshift (CB) Effect

The history of the convective blueshift effect dates back to when astronomers started investigating in detail the spectrum of the Sun, and identified disagreements between the measured line positions and their expected positions based on lab experiments (Jewell 1896; for a review see Dravins 1982). We know today that several physical processes contribute to these disagreements, one of them being the relativistic gravitational redshift (e.g., Earman & Glymour 1980). Still, even after the gravitational redshift and the Doppler shift induced by the rotation of the Sun and the Earth were accounted for the above discrepancy was not completely resolved. The corrected spectra showed that spectra of the Sun observed close to the Sun’s limb are redshifted relative to spectra from the center of the Sun’s disk,

¹Some authors use $\beta = -\lambda$ to mark this angle.

and this redshift scales with $\mu \equiv \cos \theta$, where θ is the angle between the normal to the Sun’s surface and the line of sight. This unexpected trend was studied by many (e.g., Evershed 1936; Forbes 1962; Adam et al. 1976) and its origin was a puzzle for the better part of the 20th century (for an early historic review see Forbes 1961). Before it was understood it was named the solar redshift problem, or the solar limb effect.

The solution to the problem came from the realization that the surface of a Sun-like star is composed of convective cells, or granules, where hot gas is rising upward, and cooler gas is sinking downward in the intragranular lanes. Therefore, the stellar surface is composed of local blueshifts and redshifts. Since the rising stream of hot gas is brighter than the cooler sinking gas, a net blueshift is observed (e.g., Beckers & Nelson 1978; Dravins 1982). Following the understanding of the physical process responsible for the effect it was referred to as convective blueshift. We denote the “local” blueshift velocity as V_{CB} , which is the blueshift observed at the center of the star’s disk, when averaging across a surface area larger than the size of a granulation cell. We note that the V_{CB} velocity is negative. Depending on the value of this velocity, the spectral lines are broadened in an asymmetric way and their center is shifted. For the Sun $V_{\text{CB},\odot} \approx -300 \text{ m s}^{-1}$ (e.g., Dravins 1987), and it ranges from about -200 m s^{-1} for K-type stars to -1000 m s^{-1} for F-type stars (Dravins & Nordlund 1990a; Dravins & Nordlund 1990b; Dravins 1999). For comparison the Solar gravitational redshift velocity at infinity is $+636 \text{ m s}^{-1}$ (Lindegren & Dravins 2003). Therefore, the CB effect should be accounted for when determining a star’s absolute RV, relative to its center of mass velocity (Allende Prieto et al. 2002; Lindegren & Dravins 2003; Allende Prieto et al. 2009; de la Cruz Rodríguez et al. 2011), and it should be taken into account when measuring the relative RV between the two components of a binary star, when the required accuracy is better than 1000 m s^{-1} (Pourbaix et al. 2002).

Our goal here is to quantify the impact of the CB effect on Doppler shift measurements during a planetary transit. This effect was already briefly mentioned by Winn et al. (2005), but its influence on the measured RVs was not studied.

3. The Model

We adopt a model where the planet is a spherical dark body, and the host star is a uniformly rotating spherical body with a limb darkened surface. We further assume that the host star has a uniform CB effect, where the radiation emanating from each position on its surface is blueshifted by V_{CB} directed perpendicular to the surface. A hidden assumption here is that the transiting planet size (or the stellar disk area the planet transverses during a single exposure) is much larger than the typical size of a granular cell, where for the Sun

the latter has a diameter of typically up to about 1,000 km (e.g., Roudier & Muller 1987).

We note that the adopted model is somewhat simplified as it is meant to present a first step at understanding the impact of the CB effect on spectroscopic transit observations. The model ignores possible more subtle effects (e.g., Lindegren & Dravins 2003; de la Cruz Rodríguez et al. 2011), such as meridional flows on the stellar surface (e.g., Dravins 1999), a possible different V_{CB} for different spectral lines (e.g., Dravins 1982), or at different stellar latitudes (Beckers & Taylor 1980), or a dependence of the local observed blueshift on μ (e.g., Howard et al. 1980, see also Section 4).

In our model the blueshift radial component of each surface element is μV_{CB} , so the absolute RV *decrease* induced by the CB effect is:

$$V_{0,\text{CB}} = \frac{\int_0^1 V_{\text{CB}} I(\mu) \mu^2 d\mu}{\int_0^1 I(\mu) \mu d\mu} = f V_{\text{CB}} , \quad (1)$$

where the integration is across the stellar hemisphere seen by the observer, $I(\mu)$ is the limb darkening law, and f is an order of unity coefficient. Since in our model V_{CB} is a constant we get:

$$f = \frac{\int_0^1 I(\mu) \mu^2 d\mu}{\int_0^1 I(\mu) \mu d\mu} , \quad (2)$$

which equals 2/3 when there is no limb darkening. As the granulation pattern constantly changes, the value of f will vary with a time scale of a granulation cell lifetime, which for the Sun is about 10 min (Asplund et al. 2000). However, even for short exposure times this variation is small if not negligible since it is averaged out by the integration across the stellar surface, containing many cells. Although granulation cell characteristics may change significantly for giant stars those are not targeted by high precision RV measurements. We note that the corresponding integral for the RM effect is zero when the planet is out-of-transit, meaning the origin of the RM effect — the host star rotation — does not affect the absolute RV, as expected.

As an example, we have adopted an imaginary star-planet system whose parameters are typical for a transiting system with a close-in giant planet, and are listed in Table 1. We used a planetary radius and mass of $R_p = 1.2 R_J$ and $M_p = 0.8 M_J$, and assumed a 3.5 day orbit which is completely edge-on ($i=90$ deg), circular ($e=0$) and aligned ($\lambda=0$ deg). For the host star we assumed it is a G0 type star with radius and mass of $R_s = 1.10 R_\odot$ and $M_s = 1.05 M_\odot$ (Cox 2000), rotational velocity of $V_{\text{rot}} = 2,000 \text{ m s}^{-1}$ and CB velocity of $V_{\text{CB}} = -500 \text{ m s}^{-1}$. We calculated the Keplerian orbit of such a system, and at each phase during the transit we numerically integrated over the visible and eclipsed stellar surfaces in order to calculate both the RM and CB RV shifts. We assumed a quadratic limb darkening

law and determined the coefficients using the grids of Claret (2004) for the SDSS-g' band, where the host star emits most of its radiation. In this model the coefficient f in Eq. 1 is 0.72 and $V_{0,\text{CB}} = -360 \text{ m s}^{-1}$.

The resulting RV curves are plotted in Fig. 1. The top panel shows the RV curve during transit induced by the CB effect (blue), while the RM and Keplerian signals are ignored. The middle panel shows the CB RV curve (blue) and the RM RV curve (green) and their sum (black), while ignoring the orbital RV signal. For completeness we show in the bottom panel the CB and RM RV curves including the Keplerian orbit, with the same color code as the middle panel.

4. Discussion

During transit the planet blocks light coming from different regions of the host star's surface. This changes the integrated surface area in Eq. 1, and since surface elements with different sky-projected distance from the star center have a different RV component (following a different value for μ), the result of the integration varies, giving an anomalous RV signal during transit. This signal is superposed on the Keplerian and RM signals. We note that similarly to the RM effect, the RV variation originates from a variation in the spectral line centers following a variation in their shape, and not a shift of the lines as a whole, which is the case in orbital motion. Since the CB RV shift depends only on μ (and V_{CB} , which is constant) the CB RV curve is a *symmetric* function about the mid transit time (for circular orbits).

As shown by Fig. 1 top panel, the CB effect during transit induces a small anomalous RV signal, at the 1 m s^{-1} level, although it could be larger for other stars with larger V_{CB} . The signal reaches maximum at mid transit time since in our model the observed blueshift velocity is largest close to the center of the stellar disk, which is also where most of the light coming from the star is emitted due to limb darkening.

The reason for the sign change in the CB RV curve can be understood as follows. During the transit start and end the planet blocks light coming from the stellar limb, where the radial blueshift velocity component is smaller than the average across the entire stellar disk. This in turn *increases* the overall blueshift, causing a *decrease* in the measured velocity. When the planet approaches the stellar disk center, the blueshift RV component of the eclipsed stellar surface *increases*, thereby *decreasing* the average blueshift across the rest of the disk, inducing an increase in the average velocity in Eq. 1. As seen in Fig. 1 top panel, the RV increase at mid transit is larger than the RV decrease close to transit start and end. This

reflects the geometry of the model and the limb darkened stellar surface. The maximum increase in RV can be approximated as:

$$A_{\text{CB}} \approx f V_{\text{CB}} \frac{r^2}{1 - r^2} , \quad (3)$$

where f is determined by the integrals in Eq. 2 and r is the planet to star radii ratio. For the example presented in Fig. 1, $A_{\text{CB}} = 2.3 \text{ m s}^{-1}$. We caution that Eq. 3 is a rough estimate, and A_{CB} decreases for inclined orbits with $i < 90$ deg. An order of magnitude comparison to the RM RV amplitude (Gaudi & Winn 2007, Eq. 6), gives:

$$\frac{A_{\text{CB}}}{K_{\text{RM}}} \approx \frac{V_{\text{CB}}}{V_{\text{rot}}} . \quad (4)$$

This ratio is 25 % for the example presented in Fig. 1, which uses $V_{\text{rot}} = 2,000 \text{ m s}^{-1}$, and it is larger for stars rotating more slowly. A more accurate estimate of the above ratio can be achieved by multiplying V_{CB} by f in the right hand side of Eq. 4, resulting in a ratio of 18 % for our adopted system, while the numerical integration gives a ratio of 12 %.

The CB-induced RV curve does not depend on λ or V_{rot} , meaning that on its own it does not hold information about the system’s spin-orbit alignment. In fact, the CB RV signal should be present, in principle, even if the host star does not rotate at all. Since the measured RV curve includes both effects, the CB and RM, not accounting for the CB effect in the fitted model may result in a small bias of the spin-orbit angle. This is especially true for bright host stars that are also quiet, meaning show a low stellar activity level, as those stars allow a measured RV precision comparable to and even below the amplitude of the CB-induced RV signal.

The symmetric shape of the RV curve induced by the CB effect distorts the shape of the RM signal. Specifically, for completely edge-on orbits (not necessarily aligned) or aligned orbits (not necessarily edge-on) the RM curve is an *antisymmetric* function about the mid transit time, so the combined RM + CB curve will have no definite symmetry, and the CB RV curve can not be completely absorbed into an RM model simply by changing V_{rot} or r . Therefore, the CB effect can bias the interpretation of the RV curve measured during transit and the estimate of λ . For orbits close to edge-on the distortion is strongest during the central part of the transit where it increases the measured RV. Fig. 2 presents a zoomed-in view of the middle panel of Fig. 1 around the mid transit time. It shows that the CB + RM RV curve (black solid line) crosses the RV zero point (dashed black line), meaning it equals the Keplerian velocity, later than when the RM curve does, which is at the mid transit time (dotted vertical black line), when the RM effect briefly cancels out. This time difference is approximated by dividing the CB signal at mid transit time (A_{CB}) by the slope of the RM

RV curve:

$$\Delta t \approx f V_{\text{CB}} \frac{r^2}{1-r^2} / \frac{2V_{\text{rot}} \frac{r^2}{1-r^2}}{\tau} = f \frac{V_{\text{CB}}}{V_{\text{rot}}} \left(\frac{P}{\text{day}} \right)^{1/3} \left(\frac{R_s}{R_\odot} \right) \left(\frac{M_s}{M_\odot} \right)^{-1/3} 54.4 \text{ min} , \quad (5)$$

where τ is the duration of the full transit², P is the orbital period, and M_s is the host star mass. Eq. 5 shows that the above time difference can easily be a few minutes or more. It is 6 min for the system presented in Fig. 1. Of course this time difference is dependent on the inclination angle, and for systems far from edge-on it will depend on λ as well. However, for systems close to edge-on it will depend only weakly on λ , unless λ is close to 90 or 270 deg. For example, for the system simulated here the above time difference is mimicked by the RM effect alone by increasing the impact parameter to about 0.25 and taking $\lambda \approx -15$ deg.

Therefore, an accurate estimate of the mid transit time *and* the expected Keplerian RV curve during transit are important for the correct interpretation of the spectroscopic transit RV curve and the identification of the CB effect. An accurate mid transit time can be obtained through simultaneous photometry — the measurement of the photometric light curve of the same transit event observed spectroscopically (Hirano et al. 2010; Winn et al. 2011) — since transit light curves are known to provide mid transit time estimates with an accuracy of 1 min and better. The required uncertainty on the Keplerian RV curve during transit is smaller than the CB effect amplitude. Such a low uncertainty on this RV curve can be achieved by obtaining RVs out-of-transit, both right before and right after the transit, and also on adjacent nights in orbital phases further away from the transit, to allow for an accurate orbital characterization, including specifically the RV slope during transit and the system’s center of mass velocity.

In addition, we note that for edge-on orbits with λ of 90 or 270 deg the RM signal vanishes and the in-transit RV curve will be dominated by the CB effect.

As we already mentioned the model we used here is probably a simplified version of the true behavior of the CB effect. Specifically, it was noted by several authors (e.g., Beckers & Nelson 1978; Howard et al. 1980) that the dependency of the observed local blueshift velocity scales as $\mu^\alpha V_{\text{CB}}$, where $\alpha > 1$. This leads to a faster decrease in the observed Doppler shift towards the stellar limb, faster than in the model we adopted here where $\alpha = 1$. The reason for this is the longer optical path in the stellar atmosphere closer to the limb. Using models with $\alpha > 1$ in our calculations results in increasing A_{CB} .

²The time from the second to third points of contact (Seager & Mallén-Ornelas 2003), when the planet’s disk is completely enclosed by the stellar disk.

Although beyond the scope of this paper, it is worth noting that the CB effect can influence the analysis of the RM effect in stellar binaries, where the latter is measured through a careful analysis of the variation in the spectral lines shape (Albrecht et al. 2011, and references therein).

5. Summary

We have presented here the CB effect and its impact on the RV curve during a planetary transit. We adopted a simplified model where every surface element is radiating with the same blueshift velocity, directed along the normal to the surface. Using numerical integration across the observed stellar surface we calculated the RV curves for an imaginary transiting star-planet system, similar to some of the well known transiting systems with a close-in giant planet.

The amplitude of the anomalous signal induced by the CB effect during transit is at the 1 m s^{-1} level for giant transiting planets. Not accounting for the CB effect can lead to inaccurate interpretation of the RV curve, possibly impacting the estimate of the spin-orbit angle, which will be especially visible in the case of bright and quiet host stars with accurate RVs.

For close to edge-on orbits the CB RV signal during transit is strongest at mid transit time, where it causes a time shift between the mid transit time and the time when the RV curve crosses the Keplerian curve. Therefore, an accurate estimate of the mid transit time and a well determined orbit are important for an accurate analysis of the spectroscopic transit.

So far the CB effect has been studied in detail only for the Sun. Future high-precision RVs will allow us to study it also for bright stars orbited by transiting planets, showing yet another way through which transiting planets can be used to probe their host stars. A measurement of the CB velocity for a large sample of stars will help to better understand processes such as convection and granulation, which in turn will help to better determine absolute RVs.

We are grateful to Åke Nordlund for useful discussions, and to Dainis Dravins and Eric Agol for important comments. AS acknowledges support from NASA Grant Number NNX10AG02A.

REFERENCES

Adam, M. G., Ibbetson, P. A., & Petford, A. D. 1976, MNRAS, 177, 687

Albrecht, S., Winn, J. N., Carter, J. A., Snellen, I. A. G., & de Mooij, E. J. W. 2011, ApJ, 726, 68

Allende Prieto, C., Lambert, D. L., Tull, R. G., & MacQueen, P. J. 2002, ApJ, 566, L93

Allende Prieto, C., Koesterke, L., Ramírez, I., Ludwig, H.-G., & Asplund, M. 2009, Mem. Soc. Astron. Italiana, 80, 622

Asplund, M., Nordlund, Å., Trampedach, R., Allende Prieto, C., & Stein, R. F. 2000, A&A, 359, 729

Beckers, J. M., & Taylor, W. R. 1980, Sol. Phys., 68, 41

Beckers, J. M., & Nelson, G. D. 1978, Sol. Phys., 58, 243

Claret, A. 2004, A&A, 428, 1001

Cox, A. N. 2000, Allen's Astrophysical Quantities

de la Cruz Rodríguez, J., Kiselman, D., & Carlsson, M. 2011, A&A, accepted (arXiv:1101.2671)

Dravins, D. 1982, ARA&A, 20, 61

Dravins, D. 1987, A&A, 172, 200

Dravins, D., & Nordlund, A. 1990a, A&A, 228, 183

Dravins, D., & Nordlund, A. 1990b, A&A, 228, 203

Dravins, D. 1999, IAU Colloq. 170: Precise Stellar Radial Velocities, 185, 268

Dumusque, X., Santos, N. C., Udry, S., Lovis, C., & Bonfils, X. 2010, arXiv:1011.5579

Earman, J., & Glymour, C. 1980, Stud. Hist. Philos. Sci., Vol. 11, p. 175 - 214, 11, 175

Evershed, J. 1936, MNRAS, 96, 152

Fabrycky, D., & Tremaine, S. 2007, ApJ, 669, 1298

Forbes, E. G. 1961, Annals of Science, 17, 3

Forbes, E. G. 1962, MNRAS, 125, 1

Gaudi, B. S., & Winn, J. N. 2007, ApJ, 655, 550

Hirano, T., Narita, N., Shporer, A., Sato, B., Aoki, W., & Tamura, M. 2010, PASJ, accepted (arXiv:1009.5677)

Holt, J. R. 1893 Astronomy and Astro-Physics, 12, 646

Howard, R., Boyden, J. E., & Labonte, B. J. 1980, Sol. Phys., 66, 167

Howard, A. W., et al. 2010, ApJ, 721, 1467

Jewell, L. E. 1896, ApJ, 3, 89

Li, C.-H., et al. 2008, Nature, 452, 610

Lindegren, L., & Dravins, D. 2003, A&A, 401, 1185

Lo Curto, G., et al. 2010, Proc. SPIE, 7735, 33

McLaughlin, D. B. 1924, ApJ, 60, 22

Pourbaix, D., et al. 2002, A&A, 386, 280

Queloz, D., Eggenberger, A., Mayor, M., Perrier, C., Beuzit, J. L., Naef, D., Sivan, J. P., & Udry, S. 2000, A&A, 359, L13

Rossiter, R. A. 1924, ApJ, 60, 15

Roudier, T., & Muller, R. 1987, Sol. Phys., 107, 11

Santos, N. C., Israelian, G., & Mayor, M. 2004, A&A, 415, 1153

Seager, S., & Mallén-Ornelas, G. 2003, ApJ, 585, 1038

Triaud, A. H. M. J., et al. 2010, A&A, 524, A25

Winn, J. N., et al. 2005, ApJ, 631, 1215

Winn, J. N., Fabrycky, D., Albrecht, S., & Johnson, J. A. 2010b, ApJ, 718, L145

Winn, J. N., et al. 2011, AJ, 141, 63

Table 1. Table of parameters of the transiting planetary system used in the example presented in Figs. 1 and 2.

Parameter	Value	Units
Orbital parameters:		
Orbital Period, P	3.5	day
Inclination, i	90	deg
Eccentricity, e	0	—
Spin-orbit angle, λ	0	deg
Host star parameters:		
Rotational velocity, V_{rot}	2,000	m s^{-1}
Convective blueshift, V_{CB}	-500	m s^{-1}
Star radius, R_s	1.10	R_\odot
Star mass, M_s	1.05	M_\odot
Planet parameters:		
Planet radius, R_p	1.2	R_J
Planet mass, M_p	0.8	M_J

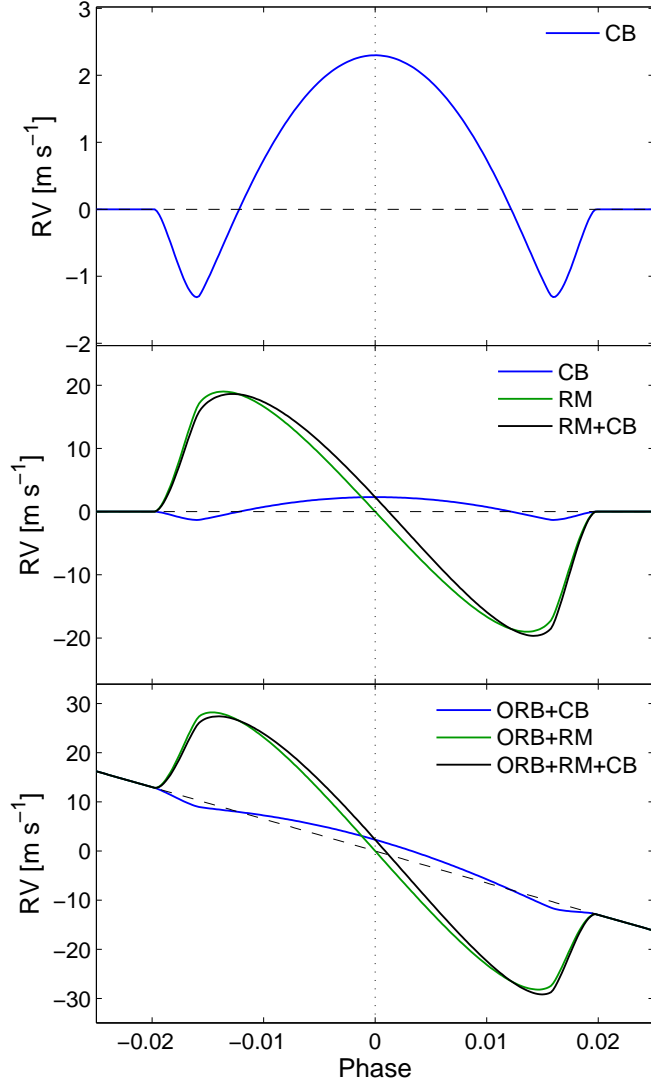


Fig. 1.— *Top*: The CB-induced RV curve during transit (blue), while the RM and Keplerian signals are ignored. *Middle*: The CB RV curve (blue) and RM RV curve (green) and their sum (black), while ignoring the Keplerian signal. *Bottom*: Similar to the middle panel, with the Keplerian orbit RV added to all three curves. All panels show RV in m s^{-1} versus orbital phase from mid transit time.

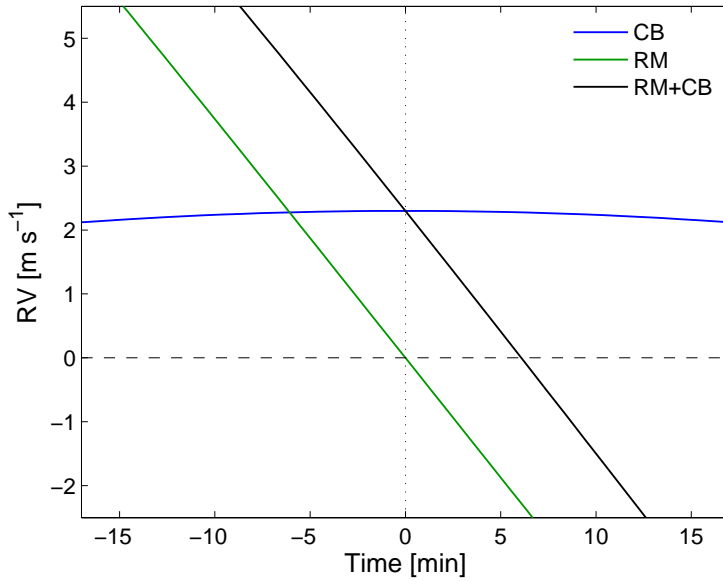


Fig. 2.— Zoomed-in view of Fig. 1 middle panel around mid transit time. The different RV curves are represented using the same color code as in Fig. 1. The figure shows that for orbits close to edge-on or spin-orbit aligned, while the RM RV effect (solid green line) briefly cancels out and crosses the zero point (dashed black line, which is equivalent to the Keplerian signal) at mid transit time (vertical dotted black line), the RV curve including the RM and CB effects (solid black line) crosses the Keplerian signal at a later time. This time difference is quantified in Eq. 5 and equals 6 min in this example. The blue solid line is the RV curve induced by the CB effect.